Available online at www.sciencedirect.com

SCIENCE DIRECT®

Journal of Solid State Chemistry 177 (2004) 1352–1358

JOURNAL OF
SOLID STATE
CHEMISTRY

http://elsevier.com/locate/jssc

Two fumarato-bridged Co(II) coordination polymers: syntheses, crystal structures and properties of $Co(H_2O)_4L$ and $[Co_3(H_2O)_4(OH)_2L_2] \cdot 2H_2O$ with $H_2L = HOOCCH = CHCOOH$

Yue-Qing Zheng* and Hong-Zhen Xie

Institute for Solid State Chemistry, Ningbo University, Municipal Key Laboratory of Inorganic Materials Chemistry, Ningbo 315211, China

Received 7 July 2003; received in revised form 11 October 2003; accepted 7 November 2003

Abstract

Two fumarato-bridged Co(II) coordination polymers $Co(H_2O)_4L$ **1** and $[Co_3(H_2O)_4(OH)_2L_2] \cdot 2H_2O$ **2** with $H_2L = HOOCCH = CHCOOH$ were prepared. Complex **1** consists of polymeric chains $^1_\infty[Co(H_2O)_4(C_4H_2O_4)_{2/2}]$, which result from octahedrally coordinated Co atoms bridged by bis-monodentate fumarate anions and are assembled by interchain hydrogen bonds. Within **2**, the edge-shared Co_2O_{10} bi-octahedra are connected to the CoO_6 octahedra to form 1D cobalt oxide chains and 3D open framework generated from the chains inter-linked by bis-bidentate fumarate anions displays rhombic tunnels, which are filled with the lattice H_2O molecules. Thermal and magnetic behaviors of both the title coordination polymers are discussed. Crystal data: (**1**) monoclinic, $P2_1/c$, $Z = 4$, $a = 7.493(1)$ Å, $b = 14.377(1)$ Å, $c = 7.708(1)$ Å, $\beta = 99.54(1)°$, $V = 818.9(2)$ Å^3, $R_1 = 0.0304$, and $wR_2 = 0.0669$ for 1487 observed reflections ($I \geqslant 2\sigma(I)$) out of 1877 unique reflections; (**2**) monoclinic, $P2_1/c$, $Z = 2$, $a = 6.618(1)$ Å, $b = 8.172(2)$ Å, $c = 15.578(3)$ Å, $\beta = 96.30(3)°$, $V = 837.4(3)$ Å^3, $R_1 = 0.0360$ and $wR_2 = 0.0663$ for 1442 observed reflections ($I \geqslant 2\sigma(I)$) out of 1927 unique reflections.

Keywords: Cobalt(II); Coordination polymer; Crystal structures; Properties

---

1. Introduction

An enormous expansion of the research field of coordination polymers based on metal-organic ligand coordination is motivated by the interest in creating structures with cavities and channels of potential use in nanotechnology, shape and size selectivity catalysis, separations and molecular recognition [1,2]. Rigid dicarboxylate ligands have been exploited to generate a variety of coordination polymers with open frameworks [3,4]. In recent years, growing attention has been paid to rational design and synthesis of coordination polymers by utilization of saturated aliphatic dicarboxylate ligands, since the flexibility and conformational freedom of such ligands could give rise to a variety of interesting structural motifs [5–11]. Among the saturated α,ω-dicarboxylate anions, the succinate ligands are of special interest. The simultaneous coordination of hydroxide and succinate groups to transition metal atoms tends to form coordination polymers with 3D open framework [12]. Compared to the succinate anions, fumarate anions exhibit less conformational freedom due to the $C=C$ double bond. To the best of our knowledge, few coordination polymers based on metal fumarato ligand have been reported yet [13]. Here, we present two new Co(II) coordination polymers, $Co(H_2O)_4(C_4H_2O_4)$ **1** and $[Co_3(H_2O)_4(OH)_2(C_4H_2O_4)_2] \cdot 2H_2O$ **2**. The Co atoms in the former are bridged by fumarato ligand into 1D polymeric chains and those in the latter are simultaneously inter-linked by hydroxo and fumarato ligands to generate a 3D open framework.

2. Experimental

All chemicals of reagent grade were commercially available and used without further purification. The C and H microanalyses were performed with a Heraeus

---

*Corresponding author. Fax: +574-87600747.
E-mail address: zhengcm@nbu.edu.cn (Y.-Q. Zheng).

doi:10.1016/j.jssc.2003.11.008

Rapid-CHNO elemental analyzer. The magnetic susceptibility was measured on a powdered sample (58.98 mg **1** and 70.98 mg **2**) using a SQUID magnetometer (Quantum Design Model MPMS-7) in a temperature range $5 \leqslant T(K) \leqslant 300$ with an applied field of 10,000 G and diamagnetic corrections were estimated from Pascal's constants [14]. The combined TG/DTA measurements were carried out from room temperature to 600°C on preweighed samples (5.24 mg **1**, 7.01 mg **2**) in a flowing nitrogen atmosphere using a Seiko Exstar6000 TG/DTA6300 equipment at a heating rate of 10°C/min.

3. Syntheses

3.1. $Co(H_2O)_4(C_4H_2O_4)$ **1**

Dropwise addition of 6.0 mL (1 M) Na_2CO_3 to a stirred aqueous solution of $CoCl_2 \cdot 6H_2O$ (0.59 g, 2.50 mmol) in 4 mL H_2O produced violet $Co(OH)_{2-2x}(CO_3)_x \cdot yH_2O$ precipitate, which was then centrifugalized and washed with double-distilled water until no Cl^- anions were detectable in the supernatant. The fresh precipitate was subsequently added to a stirred solution of 0.29 g (2.50 mmol) fumaric acid and 0.17 g (2.50 mmol) imidazole in 50 mL CH_3OH/H_2O (1:1 v/v). The mixture was further stirred for half an hour. After the insoluble solid was filtered off, the rose-colored filtrate (pH = 7.29) was maintained at 50°C and rose-colored crystals were formed in a few hours. Yields: 40% based on the initial $CoCl_2 \cdot 6H_2O$ input. *Anal.* Calc. for $C_4H_{10}CoO_8$ (%): C, 19.61; H, 4.11. Found: C, 19.58; H, 4.07.

3.2. $[Co_3(H_2O)_4(OH)_2(C_4H_2O_4)_2] \cdot 2H_2O$ **2**

A synthetic procedure analogous to **1** was used except that no imidazole was added. A rose-colored filtrate (pH = 5.46) was allowed to stand at 50°C and rose-colored crystals grew in a few hours. After the separation of the product, the pH value of the filtrate was equal to 4.83. Yields: 35% based on the initial $CoCl_2 \cdot 6H_2O$ input. *Anal.* Calc. for $C_8H_{18}Co_3O_{16}$ (%): C, 17.57; H, 3.31. Found: C, 17.52; H, 3.29.

4. X-ray crystallography

The cell determination and X-ray data collection were carried out in a Bruker P4 diffractometer with graphite-monochromated Mo*K*α radiation ($\lambda = 0.71073$ Å). The lattice parameters were refined from the 2ϑ values (10–25°) of 25 carefully centered reflections. The data with $2\vartheta_{max} = 55°$ were collected at 293 K using the $\vartheta - 2\vartheta$ scan technique and corrected for *Lp* and absorption effects. SHELXS-97 and SHELXL-97 programs [15,16] were used for structure solution and refinement. Using direct methods the structures were solved. Subsequently difference Fourier syntheses enabled all non-hydrogen atoms to be located. All hydrogen atoms of the Fumarato groups were geometrically generated while the remaining hydrogen atoms were located from the successive difference Fourier syntheses after several cycles of refinement. Finally, all non-hydrogen atoms were refined with anisotropic displacement parameters by a full-matrix least-squares technique and hydrogen atoms with isotropic displacement parameters. Detailed information about the crystal data and structure determination is summarized in Table 1. Atomic coordinates, and equivalent isotropic displacement parameters are listed in Tables 2 and 3. The selected interatomic distances and bond angles are given in Tables 4 and 5. Crystallographic data (excluding structure factors) for the structures in this paper have been deposited with Cambridge Crystallographic Data Centre as supplementary publication nos. CCDC 214504 ($C_4H_{10}CoO_8$) and CCDC 214505 ($C_8H_{18}Co_3O_{16}$). Copies of the data can be obtained, free of charge, on application to CCDC, 12 Union Road, Cambridge CB2 1EZ, UK (fax: +44 1223 336033 or mailto:deposit@ccdc.cam.ac.uk).

5. Results and discussion

5.1. Syntheses and thermal analyses

Both the title coordination polymers are synthesized under mild conditions, similar to the two cobalt succinato polymers $Co(H_2O)_4(C_4H_4O_4)$ [12c] and $[Co_3(H_2O)_4(OH)_2(C_4H_4O_4)_2] \cdot 6H_2O$ reported earlier by us [3,12b]. Férey and co-workers prepared two additional cobalt succinato polymers $Co_5(OH)_2(C_4H_4O_4)$ and $Co_4(OH)_2(H_2O)_2(C_4H_4O_4)_3 \cdot 2H_2O$ by using hydrothermal techniques [7c,7d]. The present reaction of the freshly precipitated $Co(OH)_{2-2x}(CO_3)_x \cdot yH_2O$, fumaric acid and imidazole in CH_3OH/H_2O at pH = 7.29 was originally aimed at the preparation of ternary Co imidazole fumarato complex, which serendipitously afforded a new cobalt polymeric chain compound, $Co(H_2O)_4(C_4H_2O_4)$ **1**. This fact indicates that **1** may be obtained in the absence of imidazole. To our surprise, the reaction of fresh $Co(OH)_{2-2x}(CO_3)_x \cdot yH_2O$ precipitate and fumaric acid in CH_3OH/H_2O yielded a new cobalt hydroxide fumarato coordination polymer, $[Co_3(H_2O)_4(OH)_2(C_4H_2O_4)_2] \cdot 2H_2O$ **2** at pH = 5.46. The reproducible experiments suggest that imidazole may serve as a templating reagent for the formation of **1**.

Over the temperature range 63–185°C, **1** undergoes a sharp endothermic dehydration with the observed

Table 1
Summary of crystal data, data collection, structure solution and refinement details for **1** and **2**

Compounds	**1**	**2**
Empirical formula	$C_4H_{10}CoO_8$	$C_8H_{18}Co_3O_{16}$
Formula weight	245.05	547.02
Description	Rose-colored block	Rose-colored block
Crystal size (mm)	0.22 × 0.11 × 0.11	0.20 × 0.09 × 0.07
Temperature (K)	293(2)	293(2)
Crystal system	Monoclinic	Monoclinic
Space group	$P2_1/c$	$P2_1/c$
Unit-cell dimensions		
a (Å)	7.493(1)	6.618(1)
b (Å)	14.377(1)	8.172(2)
c (Å)	7.708(1)	15.578(3)
β (deg)	99.54(1)	96.30(3)
Volume (Å^3)	818.9(2)	837.4(3)
Z	4	2
D_{calc} (g cm^{-3})	1.988	2.169
$F(000)$	500	550
μ (mm^{-1})	2.111	3.022
Absorption correction	Empirical	Empirical
Min. and max. transmission	0.396, 0.465	0.309, 0.420
θ range (deg)	2.76–27.48	2.63–27.49
Refinement method	Full-matrix least-squares on F^2	
Reflections collected	2471	2749
Independent reflections (R_{int})	1877(0.0298)	1927(0.0446)
Data/restraints/parameters	1487/0/152	1442/0/154
Goodness of fit on F^2	1.028	0.983
R_1, wR_2 $[I \geqslant 2\sigma(I)]^a$	0.0304, 0.0669	0.0360, 0.0663
R_1, wR_2 (all data)^a	0.0465, 0.0722	0.0602, 0.0732
Extinction coefficients	0.0048(9)	0.0010(5)
A, B values in weighting scheme^b	0.0307, 0.0000	0.0258, 0.0000
$\delta\rho_{max}$, $\delta\rho_{min}$ (e Å^{-3})	0.275, −0.394	0.483, −0.493

[a] $wR_2 = [\sum w(F_o^2 - F_c^2)^2 / \sum w(F_o^2)^2]^{1/2}$.

[b] $w = [\sigma^2(F_o^2) + (AP)^2 + BP]^{-1}$ with $P = (F_o^2 + 2F_c^2)/3$.

Table 2
Atomic parameters and equivalent isotropic thermal parameters (Å^2) for non-hydrogen atoms in **1**

Atom	Wyckoff site	x	y	z	U_{eq}
Co	4e	1.08085(4)	0.86039(2)	0.79994(4)	0.0161(1)
O(1)	4e	0.8850(2)	0.8350(1)	0.5762(2)	0.0227(4)
O(2)	4e	0.7314(2)	0.9681(1)	0.5505(2)	0.0266(4)
O(3)	4e	0.2670(2)	0.8760(1)	0.0327(2)	0.0224(4)
O(4)	4e	0.5276(2)	0.8665(2)	−0.0702(2)	0.0304(4)
O(5)	4e	1.0239(3)	1.0017(1)	0.7832(3)	0.0274(4)
O(6)	4e	0.8911(3)	0.8438(1)	0.9687(2)	0.0206(4)
O(7)	4e	1.1414(3)	0.7175(1)	0.8105(3)	0.0249(4)
O(8)	4e	1.2811(3)	0.8725(1)	0.6359(2)	0.0220(4)
C(1)	4e	0.7686(3)	0.8907(2)	0.4937(3)	0.0191(5)
C(2)	4e	0.6761(3)	0.8600(2)	0.3159(3)	0.0220(5)
C(3)	4e	0.5334(3)	0.9034(2)	0.2317(3)	0.0209(5)
C(4)	4e	0.4391(3)	0.8793(2)	0.0504(3)	0.0194(5)

weight loss of 29.9% corresponding well to the calculated value of 29.40% for four moles of H_2O molecules per formula unit. The formed anhydrous cobalt fumarate “Co($C_4H_2O_4$)” experiences an exothermic phase transformation at 280°C. Upon further heating, the anhydrous intermediate starts an endothermic decomposition at 380°C and finishes at 464°C, at which temperature an additional weight loss reaches 40.4% in good agreement with the calculated value of 40.01% for one mole of fumaric anhydride ($C_4H_2O_3$), and the residue collected at 600°C is identified to be CoO. When heated up to 600°C, compound **2**

Table 3
Atomic parameters and equivalent isotropic thermal parameters (Å^2) for non-hydrogen atoms in **2**

Atom	Wyckoff site	x	y	z	U_{eq}
Co(1)	$4e$	0.51578(7)	0.81829(6)	0.02371(2)	0.0141(1)
Co(2)	$2a$	1	1	0	0.0141(2)
O(1)	$4e$	0.6794(3)	0.8661(3)	0.1446(1)	0.0195(5)
O(2)	$4e$	1.0027(4)	0.8623(3)	0.1152(1)	0.0218(6)
O(3)	$4e$	1.0397(4)	0.7219(3)	0.4330(1)	0.0212(6)
O(4)	$4e$	1.3624(3)	0.7595(3)	0.4073(1)	0.0211(6)
O(5)	$4e$	0.6877(3)	0.9850(3)	−0.0361(2)	0.0140(5)
O(6)	$4e$	0.7255(5)	0.6249(4)	0.0088(2)	0.0256(6)
O(7)	$4e$	0.3406(4)	0.6601(4)	0.0960(2)	0.0224(6)
O(8)	$4e$	0.4925(5)	0.0902(5)	0.2370(2)	0.0364(8)
C(1)	$4e$	0.8685(5)	0.8459(4)	0.1650(2)	0.0173(7)
C(2)	$4e$	0.9321(5)	0.7959(5)	0.2563(2)	0.0216(8)
C(3)	$4e$	1.1093(5)	0.8293(5)	0.2978(2)	0.0212(8)
C(4)	$4e$	1.1729(5)	0.7669(4)	0.3871(2)	0.0159(7)

Note: U_{eq} is defined as one-third of the trace of the orthogonalized U_{ij} tensor.

Table 4
Selected interatomic distances (Å) and bond angles (deg) for **1**

Co–O(1)	2.103(2)	Co–O(8)	2.123(2)	C(3)–C(4)	1.499(3)
Co–O(3)$^{\#2}$	2.094(2)	C(1)–O(1)	1.274(3)	C(4)–O(3)	1.275(3)
Co–O(5)	2.075(2)	C(1)–O(2)	1.244(3)	C(4)–O(4)	1.242(3)
Co–O(6)	2.094(2)	C(1)–C(2)	1.496(3)		
Co–O(7)	2.103(2)	C(2)–C(3)	1.313(4)		
O(1)/Co/O(7)	88.78(7)	O(5)/Co/O(7)	178.44(8)	C(2)/O(2)/C(1)	119.3(2)
O(1)/Co/O(8)	89.53(7)	O(5)/Co/O(8)	92.34(8)	C(2)/O(1)/C(1)	116.5(2)
O(3)$^{\#2}$/Co/O(1)	175.14(7)	O(6)/Co/O(1)	92.07(7)	C(2)/C(1)/C(3)	121.9(2)
O(3)$^{\#2}$/Co/O(7)	87.87(7)	O(6)/Co/O(3)$^{\#2}$	84.52(7)	C(2)/C(3)/C(4)	124.8(2)
O(3)$^{\#2}$/Co/O(8)	93.76(7)	O(6)/Co/O(7)	91.65(8)	O(3)/C(4)/O(4)	124.8(2)
O(5)/Co/O(1)	90.61(8)	O(6)/Co/O(8)	177.31(8)	C(3)/O(4)/C(4)	120.3(2)
O(5)/Co/O(3)$^{\#2}$	92.83(8)	O(7)/Co/O(8)	86.22(8)	C(3)/O(3)/C(4)	114.9(2)
O(5)/Co/O(6)	89.80(8)	O(1)/C(1)/O(2)	124.2(2)		
Hydrogen bonding contacts					
D–H	d(D–H)	d(H···A)	∠(D–H···A)	d(D–H···A)	A
O(5)–H(5A)	0.77	2.18	168	2.932	O6$^{\#3}$
O(5)–H(5B)	0.83	1.93	143	2.636	O2
O(6)–H(6A)	0.73	1.97	179	2.703	O1$^{\#4}$
O(6)–H(6B)	0.85	1.87	170	2.710	O4$^{\#5}$
O(7)–H(7A)	0.81	2.07	165	2.862	O8$^{\#4}$
O(7)–H(7B)	0.80	2.03	171	2.818	O3$^{\#6}$
O(8)–H(8A)	0.85	1.86	160	2.677	O4$^{\#7}$
O(8)–H(8B)	0.78	1.93	171	2.699	O2$^{\#8}$

Symmetry codes: #1, $x-1, y, z-1$; #2, $x+1, y, z+1$; #3, $-x+2, -y+2, -z+2$; #4, $x, -y+3/2, z+1/2$; #5, $x, y, z+1$; #6, $x+1, -y+3/2, z+1/2$, #7, $x+1, y, z+1$; #8, $-x+2, -y+2, -z+1$.

experiences three endothermic processes with the peaks on the DTA curve centered at 120°C, 175°C and 424°C, respectively. The weight loss of 20.0% over 50–245°C agrees well to the calculated value of 19.76% for six moles of H_2O molecules per formula unit, and the weight loss of 40.6% over 330–500°C is slightly larger than the value of 39.14% calculated for one mole of H_2O molecule and two moles of fumaric anhydride ($C_4H_2O_3$). The residue gathered at 600°C is verified to be CoO.

5.2. Crystal structures

5.2.1. $Co(H_2O)_4(C_4H_2O_4)$ **1**

Compound **1** crystallizes isostructurally with the monoclinic $M(H_2O)_4(C_4H_4O_4)$ with M = Ni(II), Co(II) and $(C_4H_4O_4)^{2-}$ = succinate anion [12c,12d]. The Co atoms in **1** are bridged by bis-monodentate fumarate anions to generate 1D linear chains formulated as ${}^{1}_{\infty}[Co(H_2O)_4(C_4H_2O_4)_{2/2}]$ as shown in Fig. 1. The octahedral coordination environment around the Co

Table 5
Selected interatomic distances (Å) and bond angles (deg) for **2**

Co(1)–O(1)	2.103(2)	Co(2)–O(2)$^{\#1}$	2.117(2)	C(1)–C(2)	1.495(4)
Co(1)–O(4)$^{\#4}$	2.078(2)	Co(2)–O(3)$^{\#2}$	2.123(2)	C(2)–C(3)	1.304(5)
Co(1)–O(5)	2.062(2)	Co(2)–O(3)$^{\#3}$	2.123(2)	C(3)–C(4)	1.500(4)
Co(1)–O(5)$^{\#5}$	2.120(3)	Co(2)–O(5)	2.085(2)	C(4)–O(3)	1.249(4)
Co(1)–O(6)	2.133(3)	Co(2)–O(5)$^{\#1}$	2.085(2)	C(4)–O(3)	1.261(4)
Co(1)–O(7)	2.137(3)	C(1)–O(1)	1.268(4)		
Co(2)–O(2)	2.117(2)	C(1)–O(2)	1.250(4)		
O(1)/Co(1)/O(5)$^{\#5}$	92.72(9)	O(5)$^{\#5}$/Co(1)/O(7)	91.4(1)	O(5)$^{\#1}$/Co(2)/O(2)	96.51(9)
O(1)/Co(1)/O(6)	87.6(1)	O(6)/Co(1)/O(7)	90.4(1)	O(5)$^{\#1}$/Co(2)/O(2)$^{\#1}$	83.49(9)
O(1)/Co(1)/O(7)	84.1(1)	O(2)/Co(2)/O(2)$^{\#1}$	180	O(5)$^{\#1}$/Co(2)/O(3)$^{\#2}$	83.39(9)
O(4)$^{\#4}$/Co(1)/O(1)	172.9(1)	O(2)/Co(2)/O(3)$^{\#2}$	91.56(9)	O(5)$^{\#1}$/Co(2)/O(3)$^{\#3}$	90.61(9)
O(4)$^{\#4}$/Co(1)/O(5)$^{\#5}$	93.3(1)	O(2)/Co(2)/O(3)$^{\#3}$	88.44(9)	O(1)/C(1)/C(2)	116.2(3)
O(4)$^{\#4}$/Co(1)/O(6)	86.5(1)	O(2)$^{\#1}$/Co(2)/O(3)$^{\#2}$	88.44(9)	O(2)/C(1)/O(1)	125.4(3)
O(4)$^{\#4}$/Co(1)/O(7)	91.9(1)	O(2)$^{\#1}$/Co(2)/O(3)$^{\#3}$	91.56(9)	O(2)/C(1)/C(2)	118.4(3)
O(5)/Co(1)/O(1)	81.52(9)	O(3)$^{\#3}$/Co(2)/O(3)$^{\#2}$	180	C(2)/C(3)/C(4)	122.3(3)
O(5)/Co(1)/O(4)$^{\#4}$	92.8(1)	O(5)/Co(2)/O(2)	96.51(9)	C(3)/C(2)/C(1)	123.9(3)
O(5)/Co(1)/O(5)$^{\#5}$	85.9(1)	O(5)/Co(2)/O(2)$^{\#1}$	83.49(9)	O(3)/C(4)/O(4)	126.1(3)
O(5)/Co(1)/O(6)	92.4(1)	O(5)/Co(2)/O(3)$^{\#2}$	90.61(9)	O(3)/C(4)/C(3)	119.2(3)
O(5)/Co(1)/O(7)	174.7(1)	O(5)/Co(2)/O(3)$^{\#3}$	83.39(9)	O(4)/C(4)/C(3)	114.7(3)
O(5)$^{\#5}$/Co(1)/O(6)	178.3(1)	O(5)/Co(2)/O(5)$^{\#1}$			
Hydrogen bonding contacts					
D–H	*d*(D–H)	*d*(H···A)	∠DHA	*d*(D–H···A)	A
O(6)–H(6A)	0.82	1.97	167	2.797	O3$^{\#3}$
O(6)–H(6B)	0.78	2.08	172	2.850	O6$^{\#8}$
O(7)–H(7A)	0.74	2.10	168	2.722	O2$^{\#9}$
O(7)–H(7B)	0.85	1.93	177	2.694	O8$^{\#10}$
O(8)–H(8A)	0.85	2.10	155	2.893	O4$^{\#6}$
O(8)–H(8A)	0.85	1.94	150	2.711	O1$^{\#11}$

Symmetry codes: #1, $-x+2, -y+2, -z$; #2, $-x+2, 1/2+y, -z+1/2$; #3, $x, -y+3/2, z-1/2$; #4, $x-1, -y+3/2, z-1/2$; #5, $-x+1, -y+2, -z$; #6, $-x+2, y-1/2, -z+1/2$; #7, $x+1, -y+3/2, z+1/2$; #8, $-x+1, -y+1, -z$; #9, $x-1, y, z$; #10, $-x+1, y+1/2, -z+1/2$; #11, $x, y-1, z$.

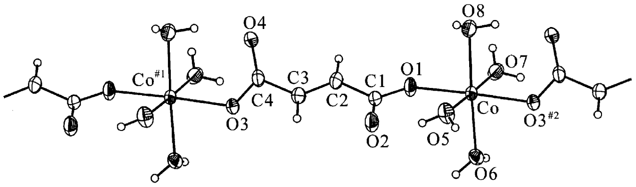

Fig. 1. Ortep view of a section of the polymeric chain $^1_\infty[Co(H_2O)_4(C_4H_2O_4)_{2/2}]$ with the atomic labelling for **1**. The displacement ellipsoids are drawn at 45% probability level (symmetry codes: see Table 4).

atoms is defined by six O atoms of four aqua ligands and two fumarate anions. The Co–O bond distances fall in the region 2.075–2.123 Å and the cisoid and transoid O–Co–O bond angles over the ranges 84.52–93.76° and 175.14–178.44°, respectively (Table 4), indicating a slight deviation of the coordination polyhedron from an ideal one. The polymeric $^1_\infty[Co(H_2O)_4(C_4H_2O_4)_{2/2}]$ chains run parallel to [101] and display two relatively strong intrachain hydrogen bonds between the aqua oxygen and uncoordinating carboxylate oxygen atoms with $d(O\cdots O) = 2.636$, 2.677 Å (Table 4). Within the crystal structure three groups of interchain hydrogen bonds exist, i.e., (1) between aqua oxygen and aqua oxygen atoms with $d(O\cdots O) = 2.862$, 2.932 Å, (2) between aqua oxygen and coordinating carboxylato oxygen atoms with $d(O\cdots O) = 2.703$, 2.818 Å and (3) between aqua oxygen and uncoordinating oxygen atoms with $d(O\cdots O) = 2.699$, 2.710 Å (Table 4). Each polymeric chain is found to be hydrogen bonded to five neighbors, which suggests that the supramolecular assembly of the polymeric chains is due to the extensive interchain hydrogen-bonding interactions. The fumarato ligand exhibits the usual bond distances and angles [13] and the carboxylato groups are found to be rotated away by 13.2(4)° and 47.4(3)°, respectively, from the plane defined by the skeleton carbon atoms due to the intrachain hydrogen bonds.

5.2.2. *$[Co_3(H_2O)_4(OH)_2(C_4H_2O_4)_2]\cdot 2H_2O$* 2

The asymmetric unit of **2** contains 14 non-hydrogen atoms, of which two are the crystallographically distinct Co atoms, namely, Co(1) and Co(2) (Fig. 2). The Co(1) atoms are in a significantly distorted octahedral environment defined by two oxygens (O(1) and O(4)) of different fumarate anions, two aqua oxygens (O(6) and O(7)) and two μ_3 hydroxo oxygens O(5) at the *cis*

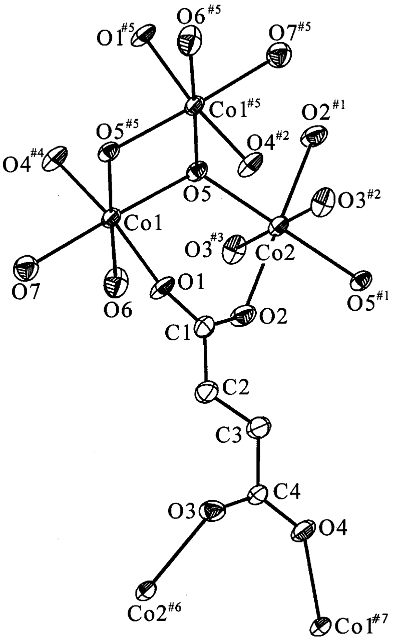

Fig. 2. Ortep view of the coordination mode of fumarato ligand and the atomic labelling for **2**. The displacement ellipsoids are drawn at 45% probability level (symmetry codes: see Table 5).

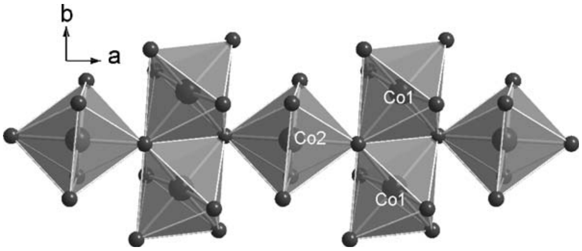

Fig. 3. 1D cobalt oxide chain generated from the edge-shared Co_2O_{10} bi-octahedra bridged by the CoO_6 octahedra in **2**.

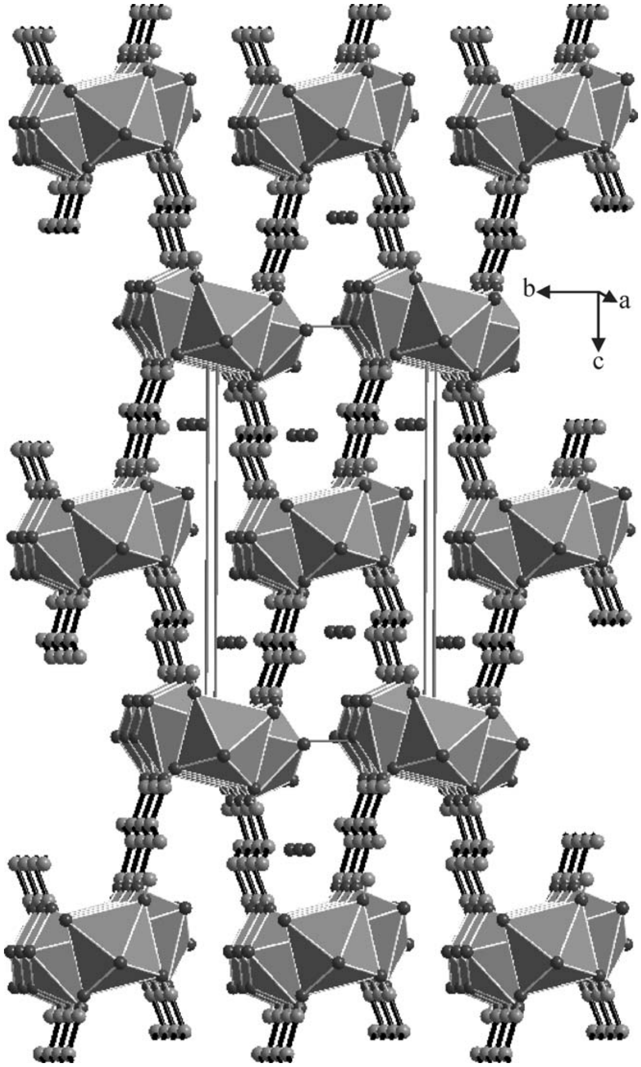

Fig. 4. Crystal structure of **2**.

positions with the Co–O bond distances in the region 2.078–2.137 Å (Table 5). Two such octahedra are condensed through two μ_3 hydroxide anions to form edge-shared bi-octahedra, which are bridged by the CoO_6 octahedra centered by the Co(2) atoms to generate cobalt oxide chain, which extends infinitely along the [100] direction (Fig. 3). The Co(2) atoms are coordinated by four oxygen atoms of different fumarate anions and two μ_3 hydroxo oxygens at the *trans* positions and the Co–O bond distances vary from 2.085 to 2.117 Å. The fumarate anions have the usual bond distances and angles [13], but the carboxylato groups are rotated away from the skeleton carbon plane by 21.3(5)° and 29.5(4)°, respectively. Through the bis-bidentate fumarate anions, the cobalt oxide chains are inter-linked into 3D open framework with rhombic tunnels propagating in the [100] direction (Fig. 4). The lattice H_2O molecules are located in the tunnels and hydrogen bonded to two carboxylato oxygen atoms with $d(O\cdots O) = 2.711$, 2.893 Å (Table 5). The present structure displays a close similarity to a cobalt succinato coordination polymer $[Co_3(H_2O)_4(OH)_2(C_4H_4O_4)_2]\cdot 6H_2O$, where the longer succinato ligands inter-link cobalt oxide chains to give larger rhombic tunnels to accommodate more water molecules [12b]. In addition, the cobalt oxide chains in the present polymer are zigzag ones and those in the latter exhibit a mirror symmetry bisecting the edge-shared bi-octahedra along the chains. Different from fumarato ligands in **2**, the non-hydrogen atoms of the succinato ligands are co-planar in the previously reported $[Co_3(H_2O)_4(OH)_2(C_4H_4O_4)_2]\cdot 6H_2O$ [12b].

According to the above description, it is now clear that the similarity of **1** to $Co(H_2O)_4(C_4H_4O_4)$ [12c] and **2** to $[Co_3(H_2O)_4(OH)_2(C_4H_4O_4)_2]\cdot 6H_2O$ [12b] is due to the similar structure of the linear dicarboxylato groups of the fumarate $(C_4H_2O_4)^{2-}$ and succinate $(C_4H_4O_4)^{2-}$ anions. Obviously, less conformational flexibility of the fumarate anions due to the C = C double bonds will not form cobalt coordination polymers with similar

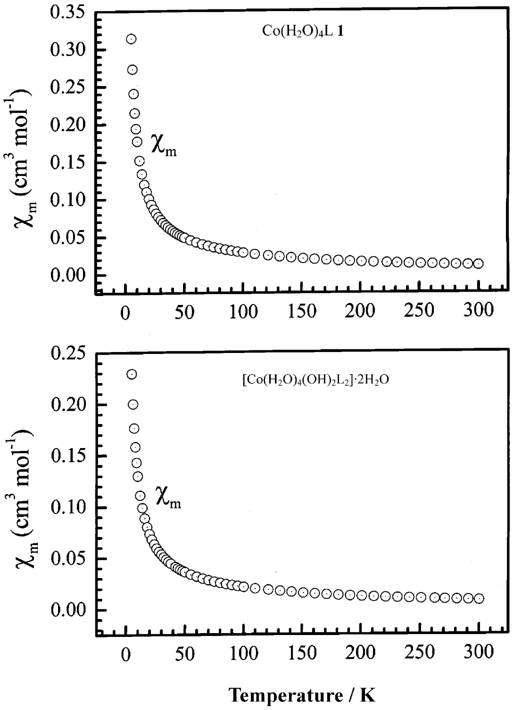

Fig. 5. The χ_m vs. T plots of **1** and **2** (χ_m being the magnetic susceptibility per Co^{2+} ion).

structures to the hydrothermally prepared $Co_5(OH)_2(C_4H_4O_4)$ and $Co_4(OH)_2(H_2O)_2(C_4H_4O_4)_3 \cdot 2H_2O$, both of which are reported to feature two-dimensional array of edge-sharing cobalt octahedra covalently linked by bent succinate anions [7c,7d]. Hydrothermal syntheses of cobalt fumarato coordination polymers are now in progress.

5.3. Magnetic properties

The temperature dependence of the magnetic susceptibility (χ_m) of **1** and **2** are shown in Fig. 5, where the χ_m is the magnetic susceptibility per molar Co^{2+} ion. For both coordination polymers, the magnetic susceptibility increases monotonously with decreasing temperature. Between 5 and 300 K, the magnetic behavior obeys the Curie–Weiss laws $\chi_m(T-\Theta) = 3.33(2)\,\mathrm{cm^3\,mol^{-1}\,K}$ with the Weiss constant $\Theta = -14.6(6)\,\mathrm{K}$ for **1** and $\chi_m(T-\Theta) = 2.52(2)\,\mathrm{cm^3\,mol^{-1}\,K}$ with the Weiss constant $\Theta = -15.4(7)\,\mathrm{K}$ for **2**. The effective magnetic moments at room temperature are 5.08 and 4.36 BM for **1** and **2**, respectively, significantly less than the spin-only value of $5.2\,\mu_B$ expected for high-spin Co(II) in an octahedral crystal field [14].

Acknowledgments

This work is supported by the National Natural Science Foundation of China (20072022), the Ningbo Minicipal Key Doctor's Funds (2003A61014) and the Ningbo Municipal Natural Science Foundation (01J20130-1). The authors are indebted to Mr. Jian-Li Lin for X-ray data collection.

References

[1] B. Moulton, M.J. Zaworotko, Chem. Rev. 101 (2001) 1629.
[2] J.-M. Lehn, Supramolecular Chemistry: Concepts and Perspectives, VCH, Weinheim, 1995.
[3] H. Li, M. Eddaoudi, M. O'Keeffe, O.M. Yaghi, Nature 402 (1999) 276.
[4] S.S.-Y. Chui, S.M.-F. Lo, J.P.H. Charmant, A.G. Orpen, I.D. William, Science 283 (1999) 1148.
[5] (a) Y.-Q. Zheng, J. Sun, J. Solid. State Chem. 172 (2003) 288;
(b) Y.-Q. Zheng, Z.-P. Kong, J. Solid. State Chem. 166 (2002) 279 (and references therein).
[6] P.M. Forster, A.K. Cheetham, Angew. Chem. Int. Ed. Engl. 41 (2002) 457.
[7] (a) C. Livage, C. Egger, M. Nogues, G. Férey, C. R. Acad. Sci. Paris: Chim. /Chem. 4 (2002) 221;
(b) C. Livage, C. Egger, G. Férey, Chem. Mater. 13 (2001) 410;
(c) C. Livage, C. Egger, G. Férey, Chem. Mater. 11 (1999) 1546;
(d) C. Livage, C. Egger, M. Nogues, G. Férey, J. Mater. Chem. 8 (1998) 2743.
[8] E. Suresh, M.M. Bhadbhade, K. Venkatasubramanian, Polyhedron 18 (1999) 657.
[9] (a) A. Michaelides, S. Skoulika, V. Kiritsis, A. Aubry, J. Chem. Soc., Chem. Commun. (1995) 1415;
(b) A. Michaelides, V. Kiritsis, S. Skoulika, A. Aubry, Angew. Chem. Int. Ed. Engl. 32 (1993) 1495.
[10] (a) M. Fleck, E. Tillmanns, L. Bohaty, Z. Kristallogr. NCS 215 (2000) 429;
(b) M. Fleck, E. Tillmanns, L. Bohaty, Z. Kristallogr. NCS 215 (2000) 619.
[11] (a) E. Lee, Y. Kim, D.-Y. Jung, Inorg. Chem. 41 (2002) 501;
(b) Y. Kim, E. Lee, D.-Y. Jung, Chem. Mater. 13 (2001) 2684;
(c) Y. Kim, D.-Y. Jung, Bull. Korean Chem. Soc. 21 (2000) 656;
(d) Y. Kim, D.-Y. Jung, Inorg. Chem. 39 (2000) 1470.
[12] (a) J.-L. Lin, Y.-Q. Zheng, J. Ningbo Univ. (NSEE) 13 (2000) 31;
(b) Y.-Q. Zheng, J.-L. Lin, Z. Kristallogr. NCS 216 (2001) 139;
(c) Y.-Q. Zheng, J.-L. Lin, Z. Kristallogr. NCS 215 (2000) 159;
(d) Y.-Q. Zheng, J.-L. Lin, Z. Kristallogr. NCS 215 (2000) 157.
[13] D.M. Young, U. Geiser, A.J. Schultz, H.H. Wang, J. Am. Chem. Soc. 120 (1998) 1331.
[14] E.A. Boudreaux, L.N. Mulay, Theory and Applications of Molecular Paramagnetism, Wiley, New York, 1976.
[15] G.M. Sheldrick, SHELXS-97, Programm zur Lösung von Kristallstrukturen, Göttingen, 1997.
[16] G.M. Sheldrick, SHELXL-97, Programm zur Verfeinerung von Kristallstrukturen, Göttingen, 1997.